Ferromagnetic-resonance studies of granular giant-magnetoresistive materials

M. Rubinstein, B. N. Das, N. C. Koon, D. B. Chrisey, and J. Horwitz
U.S. Naval Research Laboratory, Washington, D.C. 20375-5000
(Received 9 June 1993; revised manuscript received 25 January 1994)

Ferromagnetic resonance (FMR) can reveal important information on the size and shape of the ferromagnetic particles which are dispersed in granular giant magnetoresistive (GMR) materials. We have investigated the FMR spectra of three different types of granular GMR material, each with different properties: (1) melt-spun ribbons of $Fe_5Co_{15}Cu_{80}$ and $Co_{20}Cu_{80}$, (2) thin films of $Co_{20}Cu_{80}$ produced by pulsed laser deposition, and (3) a granular multilayer film of [Cu(50 Å)/Fe(10 Å)]×50. We interpret the linewidth of these materials in as simple a manner as possible, as a "powder pattern" of noninteracting ferromagnetic particles. The linewidth of the melt-spun ribbons is caused by a completely random distribution of crystalline anisotropy axes. The linewidth of these samples is strongly dependent upon the annealing temperature: the linewidth of the as-spun sample is 2.5 kOe (appropriate for single-domain particles) while the linewidth of a melt-spun sample annealed at 900 °C for 15 min is 4.5 kOe (appropriate for larger, multidomain particles). The linewidth of the granular multilayer is attributed to a restricted distribution of shape anisotropies, as expected from a discontinuous multilayer, and is only 0.98 kOe when the applied magnetic field is in the plane of the film.

I. INTRODUCTION

Granular metals, consisting of precipitates of a secondary metal in a matrix of the surrounding primary metal, have been a subject of lasting interest to both physicists and metallurgists. Granular materials are formed by admixing two otherwise immiscible metals, either by evaporating the vapors onto a cold substrate, or by rapid quenching the molten alloy onto a cold, rotating wheel. This process results in a metastable solid solution which forms larger and larger clusters of the secondary metal as the metallic admixture is annealed.

Examples of magnetic binary systems whose phase diagrams display immiscible behavior are Cu-Fe, Cu-Co, and Ag-Co. These materials first drew interest due to their Kondo-effect properties, later from their spin-glass characteristics, and quite recently from the discovery of their "giant magnetoresistance" by Xiao, Jiang, and Chien[1] and Berkowitz *et al.*[2] The magnetoresistances of these materials are remarkably large; properly prepared sputtered films of Ag-Co can exhibit a change in resistivity of more than 50% in an applied magnetic field of 8 kOe.

In this paper we are concerned with the observation of ferromagnetic resonance (FMR) in two very similar melt-spun materials which display the giant magnetoresistance (GMR) effect: $Fe_5Co_{15}Cu_{80}$ and $Co_{20}Cu_{80}$. The FMR spectra of $Cu_{70}Fe_{30}$ is also briefly considered, as is the spectrum of pulsed-laser-deposited $Co_{20}Cu_{80}$. We interpret these spectra, in as simple a manner as possible, as a "powder pattern" of noninteracting, spherical ferromagnetic precipitates, each of which resonates in an effective magnetic field composed of the applied field, the *average* dipolar field, and the randomly oriented magnetic anisotropy field. The FMR spectrum of granular solids prepared by heat treatment of multilayered samples (granular multilayers) is also considered.

As the annealing temperature of granular alloys is raised, the sizes of the individual magnetic particles increase as smaller particles coalesce and magnetic material precipitates out of solution. Ultimately, the particles will exceed the critical size for a single-magnetic-domain particle. The ferromagnetic resonance spectrum obtained from a collection of noninteracting multidomain particles will differ from a single-domain powder pattern. We have observed this transition when the Cu-Co or Cu-Co-Fe samples are annealed at about 500 °C for 15 min, at which point many of the particle diameters will grow beyond the 200 Å critical diameter for single-domain particles.

II. GIANT MAGNETORESISTANCE

In this paper we are concerned with the interpretation of ferromagnetic resonance spectra of GMR samples which have been frozen into metastable states by either melt-spinning or pulsed-laser deposition. The giant magnetoresistance phenomenon is the motivating force behind this study, and we present our GMR results at this point. Various other properties of these alloys—structure, magnetization, Mossbauer effect—have been reported elsewhere.[3]

In Fig. 1 we display the room-temperature magnetoresistance expressed as the percent change of resistance upon application of a 50-kOe magnetic field as a function of the annealing temperature for melt-spun $Fe_5Co_{15}Cu_{80}$. Melt-spun $Co_{20}Cu_{80}$ and pulsed-laser deposited (PLD) $Co_{20}Cu_{80}$, the other two materials in which we have investigated ferromagnetic resonance, behave in a similar fashion. The annealing period for each sample is 15 min. A peak in the magnetoresistance as a function of anneal temperature is observed when the samples are annealed at about 500 °C for our two melt-spun alloys, and about 400 °C for our PLD sample.

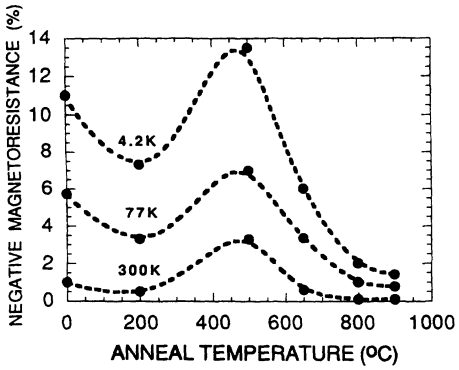

FIG. 1. Magnetoresistance ratio $\delta\rho/\rho$, expressed in percent, vs annealing temperature for melt-spun $Fe_5Co_{15}Cu_{80}$. Data are obtained at 4.2, 77, and 300 K.

The peak in the GMR upon annealing is generally attributed to the growth of the size of the ferromagnetic particles, as the smaller particles agglomerate into larger ones in these inhomogeneous, metastable alloys. The as-spun or as-deposited samples have ferromagnetic clusters which are either too small to be magnetic or are too close together to constitute an inhomogeneous alloy. The samples which are annealed at high temperatures have large particles which are too far apart to interact. It is therefore not unreasonable to expect that a maximum percent magnetoresistance can be achieved at some intermediate annealing temperature.

The reader may wonder why magnetoresistances of only a few percent are characterized as "giant." The term GMR is not merely a descriptive term but is also a technical term. It refers to a magnetoresistance which decreases with increasing magnetic field, does not depend on the direction of the applied magnetic field, and saturates with the magnetization (excluding superparamagnetism). The samples considered here satisfy all these criteria.

III. SCANNING ELECTRON MICROSCOPY

In order to visualize the structure of these samples, we display some of our scanning electron microscope photographs. Micrographs of $Fe_5Co_{15}Cu_{80}$ annealed at 500 and at 800 °C are reproduced in Fig. 2. The spun ribbon was viewed edge-on, with a magnification of 5000X. As determined by the diffraction pattern, the dark spots are images of the magnetic particles, while the light background is the Cu matrix. The top edge is the side of the ribbon which cooled in contact with the rotating hearth. The opposite side, with larger particles, is at the air interface, which cools at a slower rate. The thickness of the ribbon is 18 μm.

The distribution of particle sizes in the 500 °C sample is very inhomogeneous, and the smallest particles are much smaller than those in the 800 °C sample. The average particle size of the 800 °C sample in Fig. 2 is approximately 2000 Å, and the size distribution is more homogeneous. Very small particles are present, but not visible in these photographs. Variable-temperature magnetization measurements using a superconducting quantum interference device (SQUID) magnetometer reveal that a fraction of the particles in samples which have been annealed at lower temperatures have very small diameters. Indeed, some particles are so small that their magnetization cannot be completely saturated in 50 kOe at 4.2 K. An estimate of the radius of the superparamagnetic particles in the *unannealed* sample has been obtained from magnetization measurements, and is given in Sec. IX.

IV. FERROMAGNETIC RESONANCE

Electron-spin resonance in ferromagnetic materials (FMR) differs greatly from electron-spin resonance in

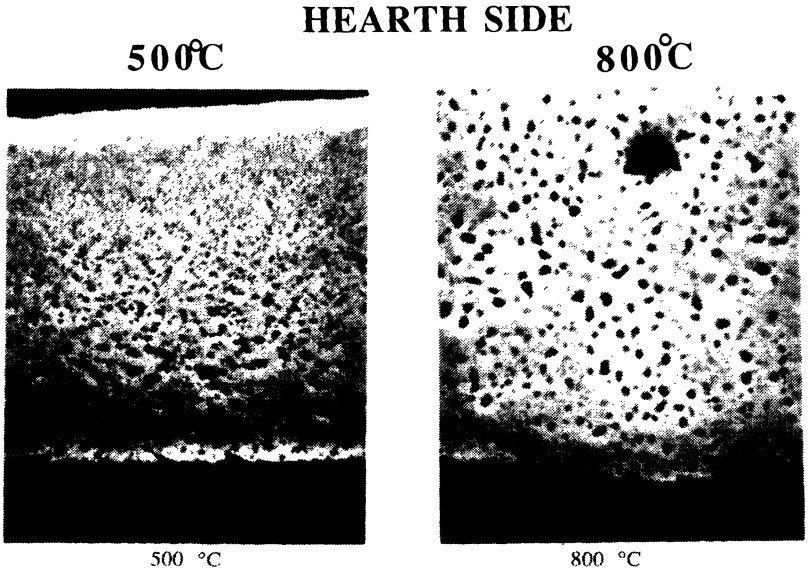

FIG. 2. Scanning electron micrograph of melt-spun $Fe_5Co_{15}Cu_{80}$ obtained for annealing temperatures of 500 and 800 °C.

nonmagnetic materials (ESR) because of the presence of large demagnetizing and anisotropy fields in ferromagnets. In the ESR case, the condition for resonance which relates the applied field H_0 and the microwave frequency of the experiment f is given by

$$f=\gamma H_0 , \tag{1}$$

where γ is the gyromagnetic ratio of the electron spins, and has the value 2.8 GHz/kOe for a free spin.

The situation is quite different when the sample is a ferromagnet. In that case, the electron-spin experiences not only the applied magnetic field but the demagnetizing field, $H_D=\underline{\underline{D}}\cdot M$, and the magnetic anisotropy field, $H_A=2K/M$. Other fields, such as the surface anisotropy field and a magnetostrictively induced field, may also be present. In the case of FMR, these additional fields are sizeable, unlike ESR, and are of the same order of magnitude as the applied field.

As Kittel[4] first showed, the condition for resonance depends on the shape of the sample because of the demagnetizing field. In the present experiment the samples are either thin foils ~ 1 mil thick and several square millimeters in area, or thin films $\sim 10\,000$ Å thick. For these samples, the external field can be placed in the plane of the sample (parallel resonance) or can be placed out of the plane and perpendicular to it (perpendicular resonance). The Kittel equations for parallel and perpendicular resonance are, respectively,

$$f/\gamma=(H)^{1/2}(H+4\pi M_{\text{eff}})^{1/2} , \tag{2a}$$

$$f/\gamma=H-4\pi M_{\text{eff}} . \tag{2b}$$

When the sample is a foil consisting of spherical inclusions of magnetic material, as is the present case, it is intuitively reasonable to use the *average* magnetization for M_{eff}. This question will be examined in more detail in Sec. XI of this paper.

Although Co and Cu are very nearly immiscible, a metastable solid solution of the two elements can be made by rapid quenching. We have produced thin melt-spun ribbons of $Fe_5Co_{15}Cu_{80}$ and $Co_{20}Cu_{80}$ by rapid quenching of the melt on a cold, rotating hearth which produces a 1-mil-thick ribbon suitable for magnetic, transport and FMR studies. We have also produced thin films of $Co_{20}Cu_{80}$ by a pulsed-laser deposition (PLD) technique, in which the ablated plume of the target is deposited onto a glass substrate. The samples were then annealed under flowing hydrogen gas for 15 min at 200, 300, 400, 500, 650, 800, and 900 °C. Magnetoresistance, magnetization, x-ray, extended x-ray-absorption fine-structure, and FMR measurements were made for many of the samples. Mössbauer-effect measurements were also performed on the $Fe_5Co_{15}Cu_{80}$ samples. A granular multilayer sample has also been investigated. Some of these results have been reported elsewhere.[3]

This paper is primarily concerned with the FMR investigations, and with the relationship of these FMR results to understanding the giant magnetoresistance phenomenon in granular alloys. The experiments were performed at both x-band and q-band frequencies, using 100-kHz field modulation, and recording the absorptive derivative lineshape. The large linewidth of the granular material rendered the 35-GHz spectra more informative than the 10-GHz spectra.

V. $Fe_5Co_{15}Cu_{80}$

Room-temperature FMR spectra were obtained at 9.5 and 35 GHz using two commercial electron-paramagnetic-resonance spectrometers. Spectra were obtained at down to 6 K, but little of interest occurred as a function of temperature. In Fig. 3 we display the 35-GHz room-temperature FMR spectra of melt-quenched $Fe_5Co_{15}Cu_{80}$. Each sample consisted of a few square millimeters of 1-mil-thick ribbon and was mounted to the wall of the microwave cavity so that the microwave magnetic field was parallel to the plane of the sample. In this geometry, the applicable Kittel equation for the value of the magnetic field necessary for resonance is given by Eq. (2a), where M_{eff} is the magnetization per unit volume averaged over the sample. For $Fe_5Co_{15}Cu_{80}$, $4\pi M_{\text{eff}}$ can be approximated by $(\frac{1}{5})4\pi M_0 \cong 3.6$ kOe (using $4\pi M_0=18$ kOe as the value of the magnetization of the alloy, Fe_5Co_{15}). Taking $f/\gamma \cong 11.7$ kOe at 35 GHz, corresponding to $g=2.2$, we obtain for the resonance field, $H=9.97$ kOe. This value agrees well with the field given by the zero crossings of the absorption derivative line shapes in Fig. 3.

The "empty" 35-GHz cavity contains several internal resonances which can distort the line shape of the samples we are interested in. This background is shown at the bottom of Fig. 3. It reflects itself in the line shape of each resonance, and must be subtracted off to obtain an accurate spectrum. This procedure will be explained below.

A better value for $4\pi M_{\text{eff}}$ can be obtained by using the *measured* value of the magnetization of the sample at the specified field and temperature. We have obtained these values using SQUID magnetometry, and the magnetization curve of $Fe_5Co_{15}Cu_{80}$ annealed at 500 °C for 15 min

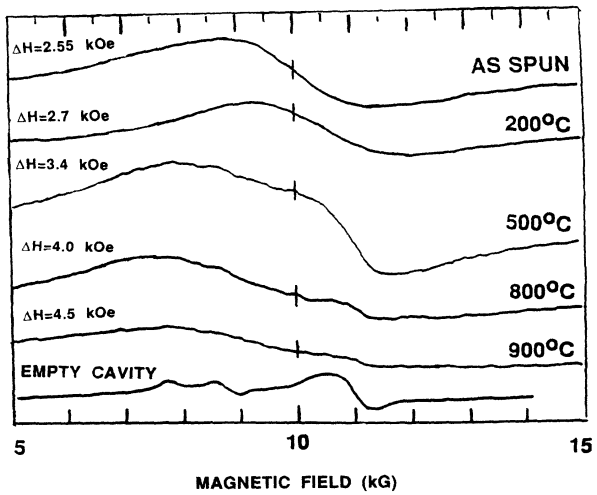

FIG. 3. Room-temperature 35-GHz FMR spectra of melt-spun $Fe_5Co_{15}Cu_{80}$ as a function of annealing temperature.

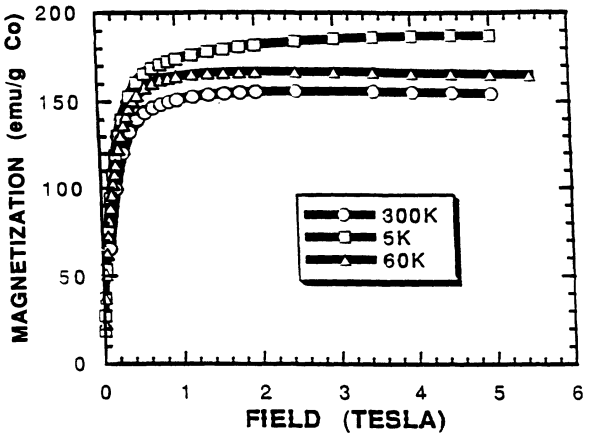

FIG. 4. SQUID magnetization curves of melt-spun granular $Fe_{56}Co_{15}Cu_{80}$ annealed at 500 °C, measured at sample temperatures of 300, 60, and 5 K.

is shown in Fig. 4 for temperatures of 300, 77, and 5 K. Using the measured value of $4\pi M$ at 300 K and 10 kOe shown in this figure, we obtain a value for the resonance field of $H_0 = 10.05$ kOe, in agreement with the estimate. FMR spectra of $Fe_5Co_{15}Cu_{80}$ taken in the perpendicular mode using Eq. (2b) are in good agreement with this value.

As an aside, we note that Fig. 4 shows that the magnetization does not saturate in the usual manner. At 4.2 K, in addition to the saturable component, a second nonsaturable component to the magnetization is evident. This component can be caused by the Co and Fe atoms which still remain in solid solution in the Cu matrix, or which form microscopic segments of γ-phase material called Guinier-Preston zones. In addition to augmenting the magnetization curve, this second phase affects the Mössbauer spectra, the x-ray spectra, and the shape of the magnetoresistance curve, making some fits to Langevin functions misleading. The FMR line shape is altered by the presence of this second phase, but it is not a dominant effect. The 300-K magnetization curve in Fig. 4 appears to saturate normally, but this is true only because, at room temperature, the paramagnetic phase becomes more pronounced at even higher fields than those shown.

The salient feature of Fig. 3 is the increase of the resonance linewidth as a function of increasing annealing time. The resonance linewidth, measured by the magnetic-field difference between the absorption derivative minimum and maximum, grows from 2.5 kOe for the as-spun ribbon to 4.5 kOe for the sample annealed at 900 °C for 15 min. The measured linewidth, determined by the field differences between the absorption derivative maximum and minimum, are noted on the spectra.

There will be some looseness to how we define the linewidth, e.g., as the half-width at half height or as the field between the extremes of the absorption derivative. The actual line shape is a convolution of the powder pattern, the intrinsic linewidth broadening function, and the distribution function of particle sizes and shapes. We have, therefore, not drawn close distinctions when they would be unwarranted.

As noted above, these spectra are marred by an extraneous background, marked "empty cavity," and shown at the bottom of Fig. 3. In Fig. 5, the sum of a Lorentzian-derivative line shape

$$f(H)=(H-H_0)/[(H-H_0)^2+(H_{1/2})^2]^2 ,$$

(where H_0 is the resonance field and $H_{1/2}$ is the half-width) and the background signal are shown. The digi-

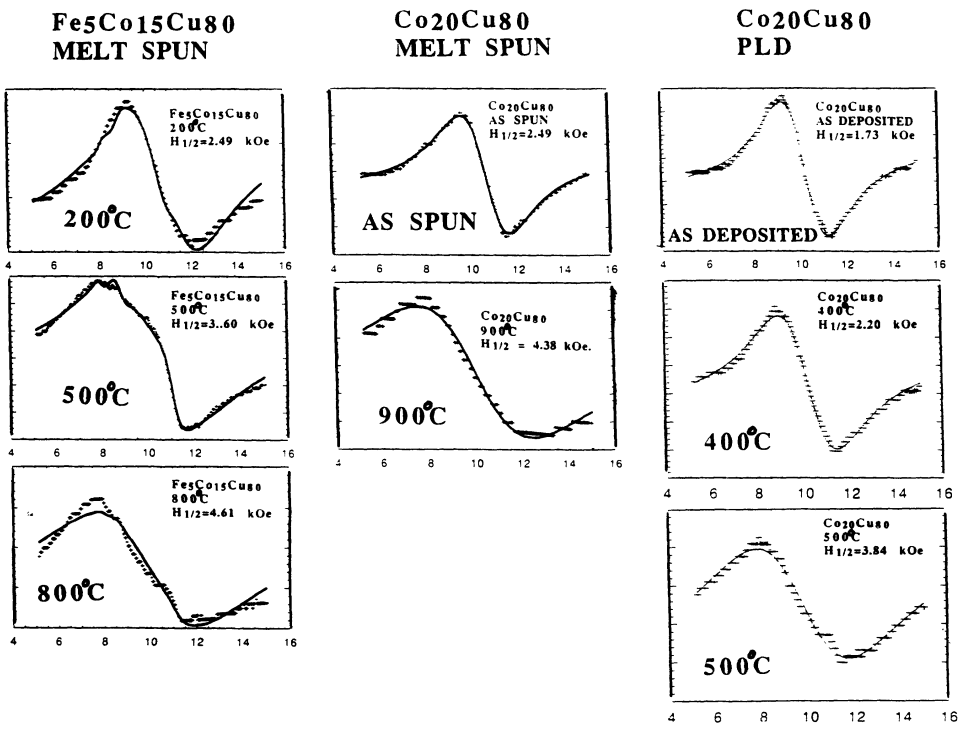

FIG. 5. FMR line shapes for melt-spun and PLD granular specimens. Crosses represent the digitized data, and solid lines are the best fit for a line shape which is the sum of the cavity background plus a Lorentzian-derivative line shape. $H_{1/2}$ is linewidth in kOe.

tized data are shown by the crosses, and the best fit to the data is shown by a solid line. This procedure shows that the structure seen in the raw spectra is primarily caused by the extraneous background, and that the true line shape can be characterized by H_0 and $H_{1/2}$, whose values are also displayed in Fig. 5. The spectra for $Fe_5Co_{15}Cu_{80}$ are in the first row of this figure. As was also evident in the spectra of Fig. 3, the linewidth increases monotonically with annealing temperature. We attribute this to the formation of multidomain particles.

VI. MULTI- AND SINGLE-DOMAIN LINEWIDTHS

Since the Co (Co-Fe) precipitates are of the order of 45 Å in the as-spun sample (Sec. IX), and grow by accretion as the annealing temperature is increased, their magnetic state will pass from small single-domain particles to that of larger multidomains. The critical diameter for a single-domain particle[4] is about 200 Å.

The crystalline and magnetic axes of these magnetic particles have no relationship to one another. Rather, they grow at random orientations, like a powder. The resulting FMR spectrum is termed a "powder pattern." Powder-pattern spectra of ferromagnetic particles have been intensively studied by Griscom[5] and co-workers. For single-domain particles Griscom and co-workers find that the linewidth

$$(\Delta H)_{SD}=(5/3)(2K/M)\ , \tag{3}$$

where K is the magnetic anisotropy energy of the particles and M is their magnetization. For a sample consisting of somewhat larger particles which have only a few domain walls, Griscom and co-workers show

$$(\Delta H)\approx 0.7(4\pi M/3)\ , \tag{4}$$

where $(\Delta H)_{MD}$ is the multidomain linewidth. For pure face-centered-cubic cobalt, $2K/M=1.2$ kOe and $4\pi M=17.9$ kOe yielding theoretical linewidths of ~ 2.0 and ~ 4.5 kOe for single-domain and multidomain linewidths, respectively, compared to the experimental values of 2.5 and 3.8 kOe obtained from Figs. 3 or 5.

VII. $Co_{20}Cu_{80}$

The FMR spectra of melt-spun and PLD ($Co_{20}Cu_{80}$ are shown in Figs. 6 and 7, respectively. The resonances were obtained at 35 GHz with both the microwave magnetic field and the applied dc magnetic field in the sample plane. Although the melt-spun and PLD samples were prepared by different techniques, both samples exhibit a monotonic change from single-domain to multidomain behavior. A distribution of particle sizes persists at high-temperature anneals; we assume that at a 900 °C anneal is sufficient to convert nearly all the particles to multidomain size.

The FMR spectra of both $Co_{20}Cu_{80}$ samples are also similar to those of $Fe_5Co_{15}Cu_{80}$. Due to the presence of Fe, the annealing behavior of $Fe_5Co_{15}Cu_{80}$ is somewhat more complex than that of $Co_{20}Cu_{80}$ when examined by x-ray diffraction. On annealing $Fe_5Co_{15}Cu_{80}$ the larger

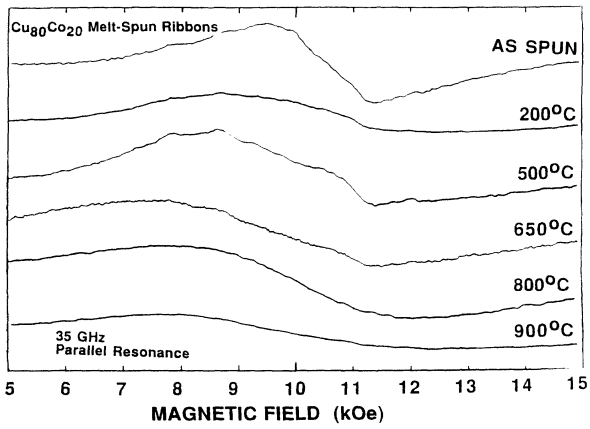

FIG. 6. Room-temperature FMR spectra of melt-spun $Cu_{80}Co_{20}$ plotted as a function of annealing temperature.

magnetic precipitates are found to have the bcc structure, while the smaller precipitates have the fcc structure of the host Cu matrix.[3] Despite these differences, the FMR spectra of $Co_{20}Cu_{80}$ are quite similar in their behavior upon annealing to that of $Fe_5Co_{15}Cu_{80}$, both becoming increasingly multidomain at high-temperature anneals. Moreover, the dependence of the GMR on annealing temperature is quite similar in both materials: each has a maximum at an annealing temperature near 500 °C. Both the FMR and the GMR dependences on annealing temperature are assumed to originate in the growth of the magnetic particles.

In Fig. 5 we display the digitized FMR line shape of the $Cu_{80}Co_{20}$ melt-spun ribbons (which are also shown undigitized in Fig. 6) for the as-spun, and 900 °C samples in the second column. We have found, by the method of least squares, the best fit to a Lorentzian derivative line shape plus the background. For the as-spun and the 900 °C sample, a simple Lorentzian derivative gave an adequate fit with $H_{1/2}=1.8$ and 4.4 kOe, respectively. Differences between the linewidths noted on Fig. 3 and

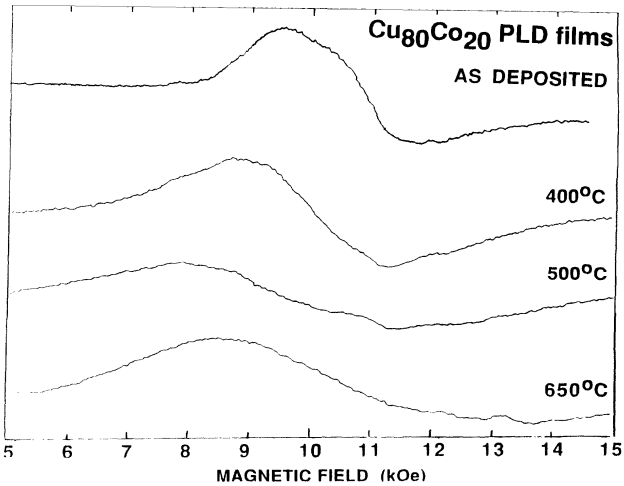

FIG. 7. Room-temperature FMR spectra of $Cu_{80}Co_{20}$ pulsed-laser deposited (PLD) thin films annealed at various temperatures.

Fig. 5 are primarily due to different definitions of linewidth, and are not significant.

Figure 7 displays the 35-GHz FMR spectra of $Cu_{80}Co_{20}$ PLD films which have been annealed at various temperatures; and the third column of Fig. 5 fits some of these to a Lorentzian derivative. Deviations from a simple Lorentzian are primarily due to extraneous background resonances.

VIII. $Fe_{30}Cu_{70}$

Not every composition will show the single-domain to multidomain transition with annealing. Melt-quenched ribbons of $Fe_{30}Cu_{70}$ showed a 35-GHz line centered around 9.0 kOe with a linewidth of 4.3 GHz, a width typical of multidomain behavior. This spectrum remained independent of annealing temperatures from the as-spun sample to the sample annealed at 900 °C for 15 min. Presumably, samples with 30% Fe are beyond the percolation threshold, and will not display single-domain magnetic behavior.

IX. DISCUSSION

Earlier, Rodbell[6] investigated the ferromagnetic resonance of the precipitated cobalt-rich phase in a 2% Co-Cu *single* crystal of Cu, as well as a thin film of Co evaporated onto a MgO single-crystal substrate. In both cases the fcc cobalt phase is stabilized by the host lattice. This sample had been heat treated to produce particles of average radius 150 Å. Since Rodbell used a single crystal, he did not observe a powder pattern caused by the random distribution of anisotropy axes, but could examine the magnetocrystalline anisotropy directly by determining the orientation dependence of the dc magnetic field required for resonance.

Rodbell found that the magnetocrystalline anisotropy field $2K/M$ for the pure Co film was 1.2 kOe, while the anisotropy field for precipitate particles in Cu-Co was 1.7 kOe. The surrounding Cu matrix stabilizes the fcc phases and increases the magnetocrystalline anisotropy. Our estimate of the single-domain linewidth expression for granular alloys, Eq. (3), may be altered by this surface anisotropy effect. Moreover, we can anticipate that the anisotropy of the individual ferromagnetic particles are actually size dependent.

The properties of granular $Fe_5Co_{15}Cu_{80}$ are somewhat different from those of $Co_{20}Cu_{80}$. We have reported elsewhere[3] that, with the addition of 25% iron to cobalt, the bcc nature of pure $Co_{75}Fe_{25}$ reasserts itself. Small particles of $Fe_5Co_{15}Cu_{80}$ are forced into registry with fcc Cu matrix by surface tension. As the particle size grows with annealing, the precipitates in $Fe_5Co_{15}Cu_{80}$ undergo a phase transition into the bcc phase. Therefore, our estimates of the magnetic parameters in $Fe_5Co_{15}Cu_{80}$ may have to be altered somewhat by these additional complexities.

Since most of the particles are single-domain at anneals below 500 °C, we now ask whether the presence of superparamagnetic particles can alter the FMR line shape. These are particles sufficiently small that thermal agitation alters their magnetic orientation. We can characterize such particles by a thermally activated magnetic relaxation time τ

$$\tau \cong f_0^{-1} \exp(CV/kT) , \tag{5}$$

where the "attempt frequency" $f_0 \cong 10^9$ sec^{-1}, V is the volume of the particle, and C is the magnetoanisotropic energy density with $C = K_1/4$ for spherical cubic particles. In order for FMR to be sensitive to superparamagnetic fluctuations, the magnetic particle must change its orientation within the "measuring time." The measuring time for FMR is determined by the 10-GHz microwave frequency and is equal to 10^{-10} sec. The relaxation time is no greater than 10^{-9} sec, and easily exceeds this limit for any temperature and volume of interest. Thus, superparamagnetism is not expected to affect FMR measurements. But GMR is affected by the absence of saturation.

We next enquire whether superparamagnetism can affect magnetoresistive measurements. For GMR materials, the measuring time is τ_{sf}, the time for a conduction electron to flip its spin. τ_{sf} is quoted to be of the order of nanoseconds,[7] a time much less than that of the superparamagnetic fluctuations. Magnetoresistance and resonance are thus both unaffected by the onset of superparamagnetism.

We have measured the zero-field-cooled magnetic susceptibility of an unannealed, as-spun sample of $Fe_5Co_{15}Cu_{80}$ as a function of temperature.[3] A maximum occurs at $T_{max} = 15$ K. This maximum occurs when the measuring time, ~ 100 sec, equals the superparamagnetic relaxation time. Using Eq. (5), with $K_1 = 4.6 \times 10^5$, we obtain $r_0 = 45$ Å as an estimate for the radius of the magnetic particles in the as-spun sample.

In Fig. 8 we plot the linewidth $H_{1/2}$ as a function of annealing temperature for $Fe_5Co_{15}Cu_{80}$, $Co_{20}Cu_{80}$ (melt-spun), and $Co_{20}Cu_{80}$ (PLD). The straight line merely indicates the trend. We assume that the as-spun and the as-deposited samples are primarily single domain, and the samples annealed at 900 °C are primarily multidomain. At intermediate anneals, the line shape can be approximated by a linear combination of the single-domain and multidomain line shapes.

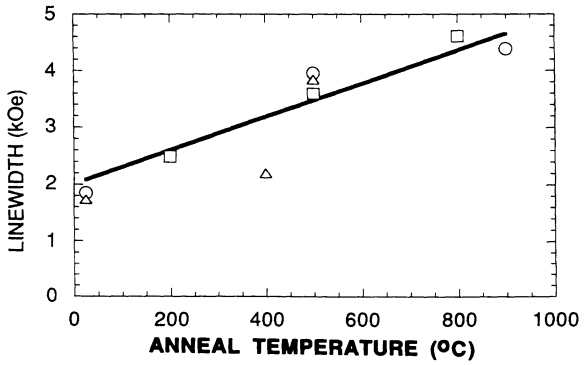

FIG. 8. FMR linewidth as a function of annealing temperature for melt-spun $Fe_5Co_{15}Cu_{80}$ (squares), melt-spun $Cu_{80}Co_{20}$ (circles), and PLD $Cu_{80}Co_{20}$ (triangles). The straight line is included to show the trend.

Finally, we discuss how the FMR measurements can aid in the interpretation of "giant" magnetoresistance in granular materials. We have already noted that magnetoresistance of Co-Cu has a maximum with respect to annealing temperature around a temperature of 500 °C. This is, coincidentally, the temperature at which FMR shows the formation of multidomain particles in our samples. Since the critical diameter for such particles is 200 Å, we can estimate that the average size of the particles are about 200 Å in our samples at the GMR maximum.

X. GRANULAR MULTILAYERS

We have investigated the ferromagnetic resonance properties of a Cu/Fe multilayer, [Cu(50 Å)/Fe(10 Å)]×50, on kapton. The sample was made by Zhang and Tejada of the University of Barcelona and was prepared by thermal evaporation in a high-vacuum system. Due, in part, to the low miscibility of Fe and in Cu, this process can produce samples with small granular particles of Fe imbedded in the Cu matrix, instead of the usual layered structures, even when the sample undergoes no post-anneal. Tejada and Zhang[8] observed a peak in the zero-field-cooled magnetization of this sample at "blocking temperature" $T_B = 150$ K, a telltale sign of the existence of small, superparamagnetic particles. Nevertheless, this sample still retains a multilayer structure, as determined by x-ray analysis. This accounts for our use of the name "granular multilayer," since these samples share attributes of both phases.

A similar process of manufacture was recently used by IBM to produce their discontinuous (granular) $Ni_{80}Fe_{20}/Ag$ multilayer films which currently hold the record for the largest sensitivity in any giant magnetoresistive (GMR) structure.[9] Although our Cu/Fe has only modest GMR our study of granular multilayers should provide insights into the magnetic structure of $Ni_{80}Fe_{20}/Ag$.

The 4.2-K magnetoresistance of the Fe/Cu granular multilayer is plotted as a function of external applied magnetic field in Fig. 9, along with the 4.2-K magnetic moment of the sample, obtained with a SQUID magnetometer. The magnetoresistance is large, decreases monotonically with field, and is independent of the field direction.

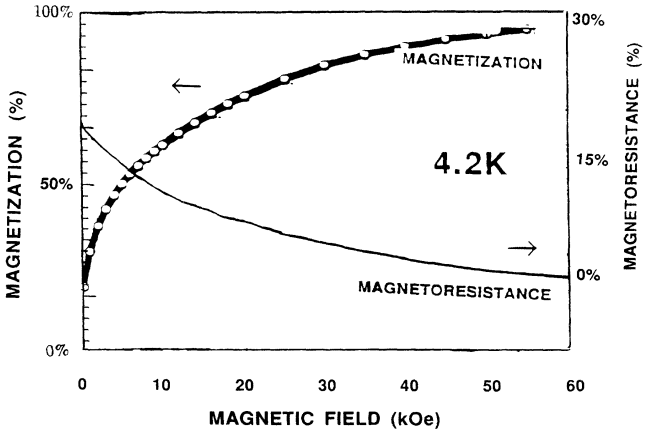

FIG. 9. Magnetization and magnetoresistance vs magnetic field at 4.2 K for Cu(50 Å)/Fe(10 Å). An easily saturable ferromagnetic component and a hard to saturate paramagnetic component are evident.

At 4.2 K and 60 kOe, the fractional change of resistance $\Delta\rho/\rho = -15\%$, but neither the magnetoresistance nor the magnetic moment is completely saturated yet. Very similar behavior is observed in the melt-spun and GMR samples. This failure to saturate is not due to ordinary magnetic hardness, or even by ordinary superparamagnetism, but is caused by the existence of a paramagnetic component, most likely Fe singlets, dimers or trimers dissolved within the Cu matrix, which coexist with the Fe precipitates. Mössbauer-effect results[8] provide substantiation for the existence of a paramagnetic fraction. The paramagnetic fraction decreases as the sample is annealed at elevated temperatures, and the size of the magnetic particles increases.

XI. FERROMAGNETIC RESONANCE AGAIN

We have obtained the ferromagnetic resonance spectrum of the Cu/Fe granular multilayer sample at 9.55 GHz with the magnetic field both parallel and perpendicular to the film plane. The spectra depend hardly at all on temperature, and the room-temperature parallel and perpendicular absorption-derivative spectra are shown in Fig. 10. The parallel resonance is centered at 1.43 kOe and has a linewidth $\Delta H_{\parallel} = 0.975$ kOe, while the perpendicular resonance is centered at 7.87 kOe with a linewidth $\Delta H_{\perp} = 1.95$ kOe. Using the Kittel equations for the Cu/Fe sample, we obtain $g = 2.18$ and $4\pi M = 4.87$ kOe. The low value of magnetization results from the low value of the iron filling factor, $\approx 20\%$. As before, we use the *average* value of the magnetization in the Kittel equations for some granular or precipitated films. Our derived values are in agreement with this conclusion, and this result will be further justified below.

The smaller linewidths of the granular multilayer compared to films and ribbons of granular $Co_{20}Cu_{80}$ and $Fe_5Co_{15}Cu_{80}$—especially that of the parallel resonance—shows that the layer formation has restricted the spread in particle orientations, constraining it to be a less-than-random distribution. We shall present some ideas on this matter, which also serve to explain why $\Delta H_{\perp}$ is so much larger than $\Delta H_{\parallel}$.

The underlying multilayer structure can distort the shape of the iron precipitates by (a) inducing uniaxial distortions in what, otherwise, would be a sphere, or (b) produce a collection of pancakelike magnetic particles aligned along the layers. These alternatives are the two extremes, neither of which may prevail in practice. The high-sensitivity NiFe-Ag granular multilayers produced by the IBM group[9] belong to group (b).

We now assume that the sample is a collection of nearly flat islandlike particles—a discontinuous multilayer. (Assuming that the particles are spheroids aligned parallel to the layer direction will not alter our quantitative conclusions, and can be treated in the same manner.) Each particle is characterized with a demagnetization tensor $\underline{N}_p$, and the thin film is characterized with a ten-

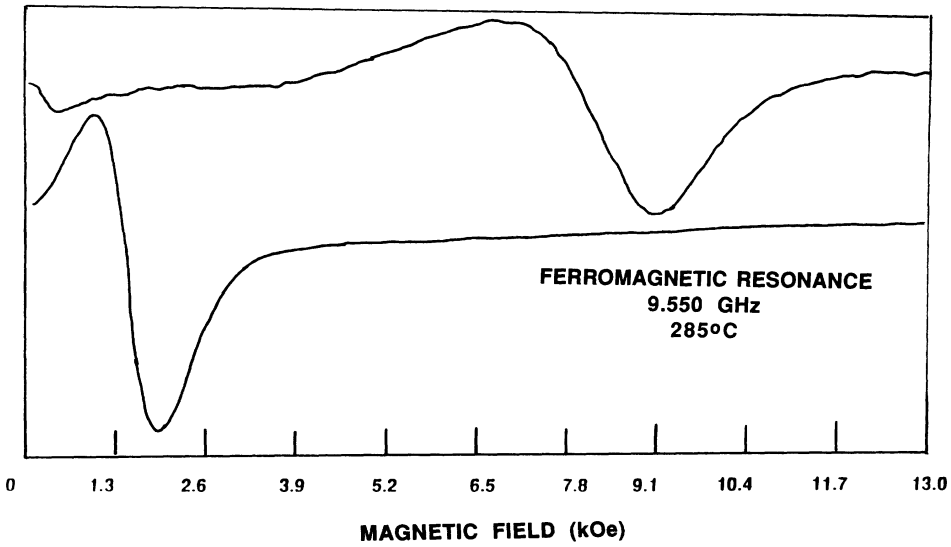

FIG. 10. 9.55-GHz FMR spectrum of Cu(50 Å)/Fe(10 Å) with applied field parallel and perpendicular to plane of film.

sor $\underline{N}_t$. Netzelmann[10] has proposed that the effective magnetostatic energy density F_N be approximated as

$$F_N=\tfrac{1}{2}(1-f)M\cdot\underline{N}_p\cdot M+\tfrac{1}{2}(f)M\cdot\underline{N}_t\cdot M\ , \tag{6}$$

where f is the volumetric filling factor of magnetic particles and M is the *particle* magnetization. Except for the constraint imposed by Eq. (2), each particle is assumed to process independently during FMR. Netzelmann[10] and Yu, Harrell, and Doyle[11] have used this approach to determine particle orientation distributions from FMR spectra in magnetic tapes.

The generalized Kittel equation, applicable to an ellipsoid with demagnetizing factors designated by N_x, N_y, and N_z, is

$$f/\gamma=\{[H_0+(N_y-N_z)M_0]\cdot[H_0+(N_x-N_z)M_0]\}^{1/2}\ , \tag{7}$$

where the z axis is always in the direction of the applied field H_0, and the γ and x axes are perpendicular to z. Choosing diagonal values $\underline{N}_p=4\pi(1-2\varepsilon,\varepsilon,\varepsilon)$ and $\underline{N}_t=4\pi(1,0,0)$, appropriate to an ellipsoidal particle and a thin film, respectively, we obtain the following values for the Kittel demagnetizing factors, for parallel and perpendicular resonance (see Table I).

TABLE I. Values for the Kittel demagnetizing factors for parallel and perpendicular resonance.

Effective demagnetizing factor	Perpendicular resonance	Parallel resonance
N_z	$4\pi f+4\pi(1-f)(1-2\varepsilon)$	$4\pi(1-f)\varepsilon$
N_x	$4\pi(1-f)\varepsilon$	$4\pi f+4\pi(1-f)(1-2\varepsilon)$
N_y	$4\pi(1-f)\varepsilon$	$4\pi(1-f)\varepsilon$

We now assume that the FMR linewidth is primarily caused by a flat distribution of particle ellipticity parameters, ε, which vary between $\varepsilon=0$ and $\varepsilon=\varepsilon_0$. Using Eq. (2), the perpendicular resonance linewidth is given by $\Delta H_\perp=4\pi M_0\varepsilon_0(1-f)$, from which we obtain the value $\varepsilon_0=0.12$ from the experimental value of the perpendicular linewidth, $\Delta H_\perp=1.95$ kOe. The Netzelman-Kittel equation yields $\Delta H_\parallel=0.65$ kOe for the value of the parallel resonance linewidth, (compared to the experimental value of 0.97 kOe), and shows why the parallel resonance linewidth differs than from the perpendicular resonance linewidth.

Using nearly spherical particles with a distribution of ellipsoidal distortions, instead of pancake-shaped particles, yields the same quantitative conclusions. However, using nearly spherical particles results in a larger discrepancy in the ratio of the two linewidths than using nearly flat particles. However, from FMR linewidths alone, we are hesitant to draw too many conclusions. Other[9] granular multilayer systems are found to have flat, islandlike precipitates. We conclude that our sample probably consists of a collection of flat ellipsoids. Each ellipsoid has a unique ellipticity parameter ε, and they are distributed fairly evenly between the value $\varepsilon=0$ and $\varepsilon=0.12$.

Netzelman's formula can be used to confirm that the effective value of magnetization to be used in Kittel's equations [Eq. (2)] for a granular thin film composed of magnetic spherical particles immersed in a nonmagnetic matrix is the *average* magnetization. For spherical particles imbedded in a thin film, setting the diagonal values $N_p=4\pi(\frac{1}{3},\frac{1}{3},\frac{1}{3})$ and $N_t=4\pi(1,0,0)$, we obtain from Eqs. (6) and (7), $M_{\text{eff}}=fM$. Here, f is the volume percentage of the precipitate and M is the magnetization of the particles. Similar conclusions are reached in work on ferromagnetic resonance of implanted spherical particles of metallic α iron in fused silica.[5] It is there termed the *independent particle approximation*, but the works of

Netzelmann[10] and Yu, Harrell, and Doyle[11] indicate its validity for higher concentrations of magnetic particles than this name would imply.

In summary, we have investigated the linewidth mechanisms of some melt-spun, vapor-deposited, and annealed-multilayer granular materials. We conclude that both the size and the shape of these particles have a pronounced effect on the linewidth. These same parameters—size and shape—also determine the magnitude of the giant magnetoresistance.

[1]J. Q. Xiao, J. S. Jiang, and C. L. Chien, Phys. Rev. Lett. **68**, 3749 (1992).

[2]A. E. Berkowitz *et al.*, Phys. Rev. Lett. **68**, 3745 (1992).

[3]V. G. Harris, B. N. Das, M. Rubinstein, J. L. Goldberg, W. T. Elam, and N. C. Koon, IEEE Trans. Magn. (to be published); M. Rubinstein, B. N. Das, and N. C. Koon, J. Appl. Phys. **73**, 5540 (1993) (abstract only); V. G. Harris, M. Rubinstein, and B. N. Das, J. Appl. Phys. (to be published).

[4]C. Kittel, *Introduction to Solid State Physics,* 6th ed. (Wiley, New York, 1986), p. 47; in *Solid State Physics,* edited by Frederick Seitz and David Turnbull (Academic, New York, 1956), Vol. 3; C. Kittel, Phys. Rev. **73**, 155 (1948).

[5]D. L. Griscom, C. L. Marquardt, E. J. Friebele, and D. J. Dunlop, Earth Planet. Sci. Lett. **24**, 78 (1974); D. L. Griscom *et al.*, Nucl. Instrum. Methods Phys. Res. Sect. B **32**, 272 (1988); D. L. Griscom, J. Non-Cryst. Solids **67**, 81 (1984).

[6]D. S. Rodbell, J. Appl. Phys. **19**, 311 (1958); J. Phys. Soc. Jpn. **17**, 313 (1962).

[7]P. C. von Son, H. van Kempen, and P. Wyder, Phys. Rev. Lett. **58**, 2271 (1987).

[8]J. Tejada *et al.*, J. Magn. Magn. Mater. **93**, 425 (1991); (private communication).

[9]T. L. Hylton, K. R. Coffey, M. A. Parker, and J. K. Howard, Science **261**, 1021 (1993).

[10]U. Netzelmann, J. Appl. Phys. **68**, 1800 (1990).

[11]Y. Yu, J. W. Harrell, and W. D. Doyle, J. Appl. Phys. (to be published).

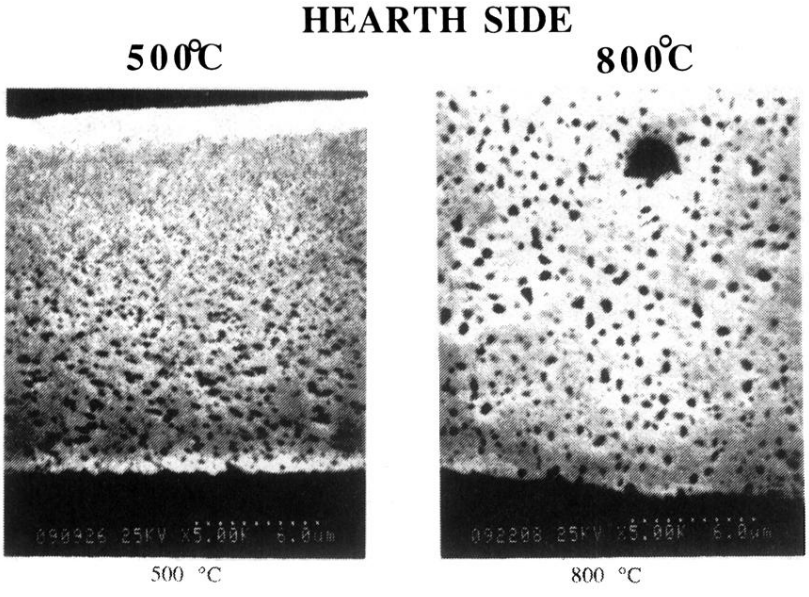

FIG. 2. Scanning electron micrograph of melt-spun $Fe_5Co_{15}Cu_{80}$ obtained for annealing temperatures of 500 and 800 °C.